The Seoul Journal of Medicine
Vol. 28, No. 4:353-367, December 1987

High Field (2.0T) MRI in Sellar and Juxtasellar Lesions[1]

Kee Hyun Chang[2], Moon Hee Han, Byung Kyu Cho*, Dae Hee Han*, Kil Soo Choi*, Man Chung Han, Ho-Jin Myung** and Chu-Wan Kim

Departments of Radiology, Neurosurgery and Neurology**, College of Medicine, Seoul National University, Seoul 110, Korea*

= Abstract =We prospectively evaluated the magnetic resonance (MR) images of 28 sellar and juxtasellar lesions which were obtained using a 2.0T superconducting MR system and compared them with computed tomography (CT) scans. A variety of lesions were included: 14 pituitary adenomas; three germ cell tumors; two each of meningioma and empty sella; and one each of craniopharyngioma, teratoma, epidermoid, trigeminal neuroma, nasopharyngeal cancer with parasellar extension, tuberculoma and carotid cavernous fistula (CCF). MR more clearly demonstrated the relation of the lesions with the optic chiasm, infundibular stalk, carotid arteries, 3rd ventricle and cavernous sinus. Carotid and cavernous vascular structures were better evaluated with MR, and angiography may be avoided in some cases. MR enabled characterization of lesions containing hemorrhage, fat and flowing blood, and allowed more specific diagnoses than CT in hemorrhagic tumor and CCF. MR was equivalent to CT in detecting the lesions, even though most of the homogeneously enhancing tumors on CT including pituitary adenomas, meningiomas, germ cell tumors, tuberculoma, etc, revealed isointensity signal on MR. CT was more sensitive than MR for detecting calcification and sella-floor erosion.

Key words: ***Magnetic resonance imaging (MRI), Brain tumor, Pituitary tumor, Juxtasellar tumor***

INTRODUCTION

The investigation of pituitary pathology has undergone significant changes during the past two decades. In the mid-1970s, computed tomography (CT) replaced pleuridirectional tomography, pneumoencephalography, and angiography. CT permitted direct visualization of the sella turcica and its soft tissue contents in a non-invasive manner (Davis *et al.* 1985). Magnetic resonance (MR) imaging now offers significant advantages over CT without intravenous contrast or radiation exposure and is widely accepted as an effective modality in the evaluation of a variety of intracranial abnormalities and provides superior contrast sensitivity and delineation of vascular structures, qualities that are of special importance in the suprasellar region (Karnaze *et al.* 1986). It has been suggested that MR imaging may be more effective than CT in several studies of primarily sellar lesions, including some parasellar abnormalities (Oot *et al.* 1984; Bilaniuk *et al.* 1984a; Lee *et al.* 1985; Karnaze *et al.* 1986). Early MR systems with low magnetic fields were only capable of relatively coarse spatial resolution, typically 7-to 15-mm-thick sections and pixel sizes over 1 mm. Such resolution was simply inadequate for the evaluation of small lesions or intricate anatomy. With the current generation of MR systems, much improved spatial definition is possible. Modern units with high magnetic field can provide contiguous 3-to 4-mm-thick sections and pixel sizes less than 1 mm with routine multislice two-dimensional Fourier transform (2 DFT) technique. Three-dimensional Fourier transform (3 DFT) techniques allow even thinner slices (1.5 mm or less) but are less commonly used, primarily because they are more time consuming

[1]This study was supported in part by the clinical research grant of Seoul National University Hospital (1987).

[2] Author for correspondence.

(Bilaniuk *et al.* 1984b; Kucharczyk *et al.* 1986; Kucharczyk 1987). In 1985 a superconducting MR system operating at a high magnetic field (2.0 Tesla) was developed by Korea Advanced Institute of Science and Technology (KAIST), Seoul, Korea. To determine if and how 2.0T MR provides any significant new information in the evaluation of sellar and juxtasellar lesions, a comparative study of MR imaging and CT was performed.

MATERIALS AND METHODS

Between May 1986 and July 1987, twenty-eight patients with sellar and juxtasellar lesions were studied by both CT and MR. Patients ranged in age from 9 to 67 years; 18 were females, and 10 were males. There were 16 primary sellar lesions: 14 pituitary adenomas and two empty sellae. Twelve were juxtasellar lesions: 3 germ cell tumors, 2 meningiomas and one each of craniopharyngioma, trigeminal neuroma, teratoma, epidermoid, tuberculoma, carotid-cavernous fistula and parasellar extension of nasopharyngeal cancer. Pathologic proof was obtained in 21 cases. Two each of macroadenoma and empty sella, one each of microadenoma, tuberculoma and CCF were not pathologically proved. These were firmly diagnosed on the basis of clinical, laboratory and radiological findings. Arteriography was performed in selected cases to evaluate the carotid arteries.

MR imaging was performed with a 2.0T superconducting unit developed by Korea Advanced Institute of Science and Technology (KAIST). Multislice coronal and sagittal spin-echo (SE) sequences using echo times (TE) of 30 or 60 msec, and repetition times (TR) of 500 or 2,000 msec — SE 500/30, 2000/30, 2000/60 — were performed in nearly all cases.

All images were obtained by the two-dimensional Fourier transform method. The number of averages was two or four, and section thickness was 4 mm for small pituitary lesions and 5 to 10 mm for the others, with 0-1 mm gap. The acquisition matrix was 256 × 256, corresponding to spatial resolution of 1 mm × 1 mm. In 4 selected patients with small pituitary adenomas, three-dimensional Fourier transform method was utilized for thin slice thickness (2 mm).

CT scanning was performed with either GE 9800 or 8800 scanners with 1.5 or 5 mm contiguous sections for the pituitary lesions and 5 mm or 10 mm sections for juxtasellar lesions in the axial and/or coronal planes.

MR signal intensity of the lesion was described as hyperintense, isointense, or hypointense relative to that of the brain cortex. Images were compared to evaluate the ability of CT and MR to detect and characterize lesions, to detect sella-floor erosion, and to define the relationship of lesions to the optic chiasm, infundibulum, carotid arteries, and cavernous sinus.

Cavernous sinus invasion on CT was suspected when the lateral margin of the cavernous sinus bowed outward or was grossly asymmetric. By MR, cavernous sinus invasion was suspected on the basis of displacement of the lateral margin of the cavernous sinus, displacement of the cavernous internal carotid artery, or a change in intensity pattern of the cavernous sinus tissue to one similar to the adjacent sellar mass.

RESULTS

All of the pituitary abnormalities were well shown by both contrast-enhanced CT and by high field MR imaging. However, high field MR images better demonstrated the anatomic relationships of the lesions, particularly their relationship to the chiasm, infundibulum and the intracavernous carotid arteries.

Sagittal MR images proved better than coronal images in depicting the antero-posterior relationship of the mass to the optic chiasm, infundibulum and brainstem. Cronal images were superior in evaluating the carotid arteries and third ventricle.

Optic chiasm compression was identified convincingly in all patients with MR. In several cases, chiasmal compression was suspected with CT on the basis of size of the adenoma; however, the optic chiasm was not adequately defined with CT for confirmation.

The signal intensity of the lesions was summarized in Table 1. Of fourteen pituitary adenomas (12 macroadenomas and 2 microadenomas) nine (8 macroadenomas and 1 microadenoma) were purely solid tumors, three had hemorrhagic necrosis within the tumor, and two showed cystic changes. These findings were based on the surgical and pathologic findings in 11 cases and were based on clinical, CT and MR findings in remaining 3 cases. Of the three adenomas with no surgical proof, two were macroadenomas showing homogeneous enhancement on CT and another was a microadenoma which showed decreased size of the pituitary mass, decreased CT density

Table 1. Signal intensity of the tumors

Seq. / Diagnosis (No.)	T1WI	Balanced	T2WI
Pituitary adenoma (14)	→(12) ↑(2)	→(7) ↑(2)	→(6) ↑(4)
cystic portion	↓(2)	↕	⬇
hemorrhagic portion	⬆(3)	⬆(3)	⬆(3)
Germ cell tumor (3)	→(3)	→(2)	→(1) ↑(1)
surrounding edema	→(1)	⬆(1)	⬆(1)
cystic portion	↓(1)	→(1)	⬆(1)
Meningioma (2)	→(2)	→(1)	↑(1)
Craniopharyngioma (1)	↑	↑	⬆
Epidermoid (1)	⬇		⬆
Teratoma (1)	⬆	⬆	↑
Trigeminal neuroma (1)	→		↑
hemorrhagic portion	⬆		⬆
Tuberculoma (1)	→	→	→
surrounding edema	→	↑	⬆
Nasopharyngeal cancer (1)	→	→	→
CCF (1)	⬇	⬇	⬇

→: isointense
↑: slightly hyperintense
⬆: markedly hyperintense
↓: slightly hpointense
⬇: markedly hypointense
↕: hyperintense supernatant and hypointense precipitate

and high MR signal intensity after bromocriptine therapy, suggesting hemorrhagic change.

Seven of 9 solid adenomas were isointense and 2 were slightly hyperintense on T1-weighted images (SE 500/30) (Fig. 1). Among the 7 patients with solid adenoma examined with balanced (SE 2000/30) and T2-weighted (SE 2000/60) sequences, 5 were isointense and 2 were slightly hyperintense on balanced images, while 4 were isointense and 3 were slightly hyperintense on T2-weighted images. Two macroadenomas associated with empty sella revealed isointense masses within the sphenoid sinus in all sequences. Three adenomas with hemorrhagic necrosis were markedly hyperintense on all sequences (Fig. 2). MR imaging was superior to CT in these cases because it provided better differentiation of a hemorrhagic necrosis from cystic change, while CT showed hypodense mass in either one. Calcification in the wall of one hemorrhagic adenoma appeared as slightly hopointense in all sequences. Cystic portions of two adenomas varied in MR intensity; one revealed slight hypointensity on SE 500/30 images and isointensity on SE 2000/60 images. Another cystic adenoma had fluid level, in which supernatant was isointense on SE 500/30 and markedly hyperintense on SE 2000/60 images, while precipitate were hypointense on all sequences. One surgically proven solid microadenoma demonstrated slight hyperintensity on all sequences (Fig. 3).

Eight solid adenomas were homogeneous in appearance, and one was slightly inhomogenous with focal areas of hyperintensity on T1-weighted images.

Extension of adenomas into the cavernous sinus was suspected by MR in eight patients (Fig. 4), compared with six patients who were suspected of having cavernous sinus abnormalities by CT. Cavernous sinus invasion was not surgically confirmed due to inaccessibility of the cavernous sinus. As shown in Fig. 4, the tumor with suprasellar and right cavernous extension was equally well visualized on MR images with both 4 mm and 2 mm thickness, even though 2 mm-thick images showed more noise than 4 mm-thick images.

Subarachnoid space with the same signal intensity as CSF was seen extending into the sella in sagittal and coronal sections of two cases with empty sella. The pituitary stalk was clearly seen in two cases on SE 500/30; one was eccentric in location. The diagnosis was made with the same accuracy on thin coronal CT as on MR images.

Fig. 1. Pituitary adenoma with suprasellar extension. Note isointense signal of the tumor on SE 500/30 and good delineation of the relationship to perisellar structures.

The germ cell tumors showed isointensity on T1-weighted images (SE 500/30) in all 3 cases (Fig. 5). On balanced (SE 2000/30) and T2-weighted (SE 2000/60) images examined in 2 patients, the signal of mass was isointense in both sequences in one patient, while it was isointense on balanced image and slightly hyperintense on T2-weighted image in another patient. The surrounding edema found in one case revealed isointensity on SE 500/30 and hyperintensity on both SE 2000/30 and 2000/60 images. The cystic portion of the mass was found in one patient, showing hypointensity, isointensity and hyperintensity on T1-weighted, balanced and T2-weighted images, respectively. Post-contrast CT better demonstrated tumor contrast than MR, whereas MR revealed better anatomic detail in both sagittal and coronal sections.

One of two meningiomas was parasellar, and another was suprasellar in location. The signal was isointense on SE 500/30 (Fig. 6) and 2000/30 sequences in both cases, but in T2-weighted sequence (SE 2000/60) it was mildly hyperintense in one and isointense in another. The MR images of the suprasellar meningioma failed to differentiate the mass from normal brain tissue because of isointense signal and dense adhesion to the normal brain tissue and failed to demonstrate bony hyperostosis of tuberculum sella seen on CT. CT was more diagnostic in this case and was superior to MR because of high contrast sensitivity and hyperostosis. Detailed anatomy of perisellar area, however, was better seen with MR. In the smaller parasellar meningioma, CT demonstrated a highly enhancing mass but failed to exclude the possibility of carotid aneurysm, but the normal carotid artery was precisely evaluated with MR.

The signal of a craniopharyngioma was slightly

Fig. 2. Pituitary adenoma with hemorrhagic necrosis. Post-contrast CT scan (A) shows multiple low density within the tumor, which could not differentiate the cystic change from hemorrhagic necrosis. MR image of SE 500/30 (B) demonstrates hemorrhagic area of high signal intensity.

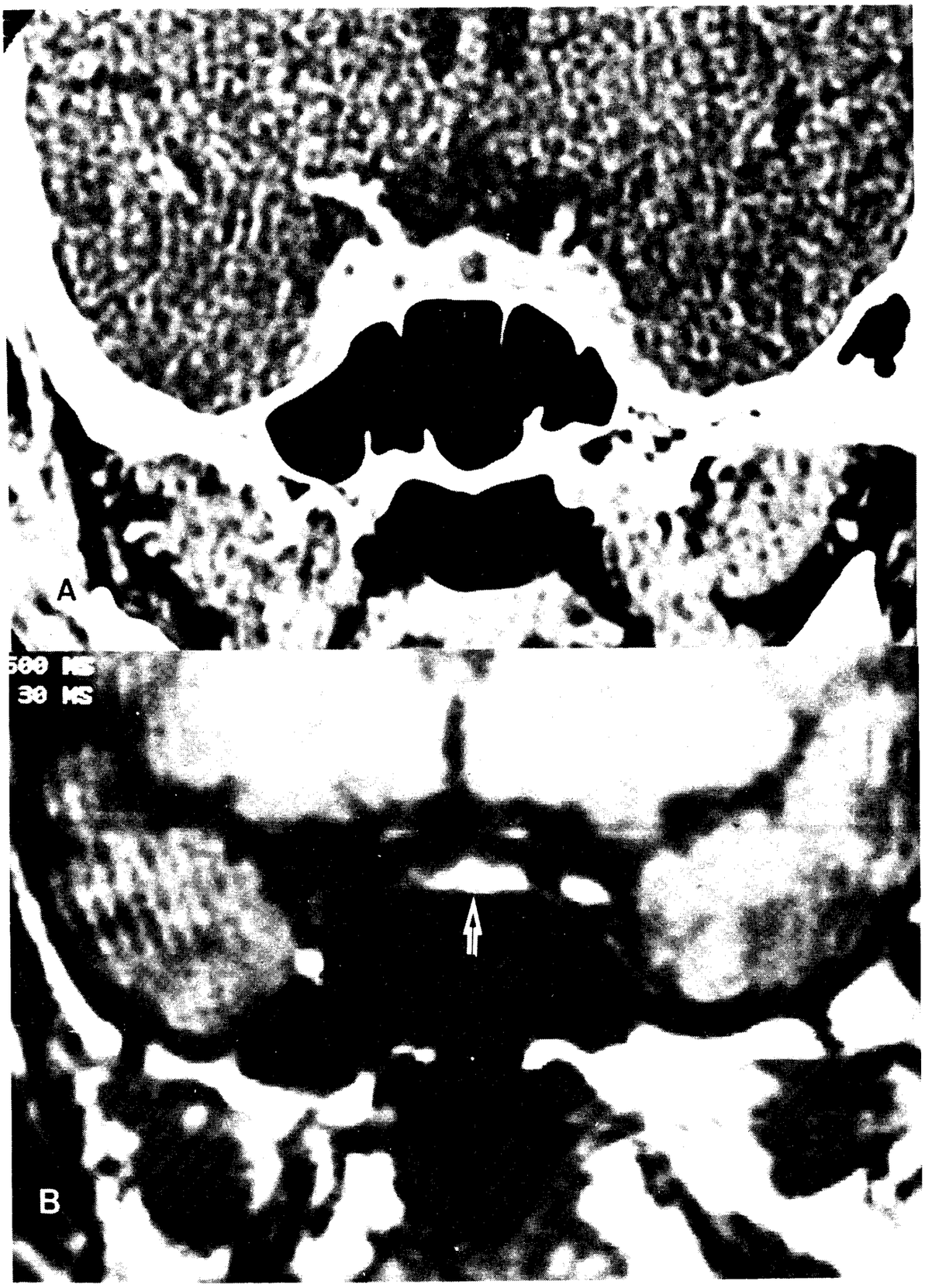

Fig. 3. Pituitary microadenoma with Cushing syndrome. Post-contrast CT (A) shows small (approximately 4 mm × 4 mm) round mass of low density within the central portion of the gland. MR (SE 50/30) (B) image reveals less distinct small round mass of high signal intensity at same area (arrow).

Fig. 4. Pituitary adenoma with extension to suprasellar area and right cavernous sinus. Both MR (SE 500/30) images of 4 mm- (A) and 2 mm- thickness (B) reveal slightly heterogenous signal intensity of the tumor, and extension to suprasellar area and right cavernous sinus, displacing right carotid artery downward. Note granular noisy apperance on 2 mm-thick image (B) due to lower signal to noise ratio.

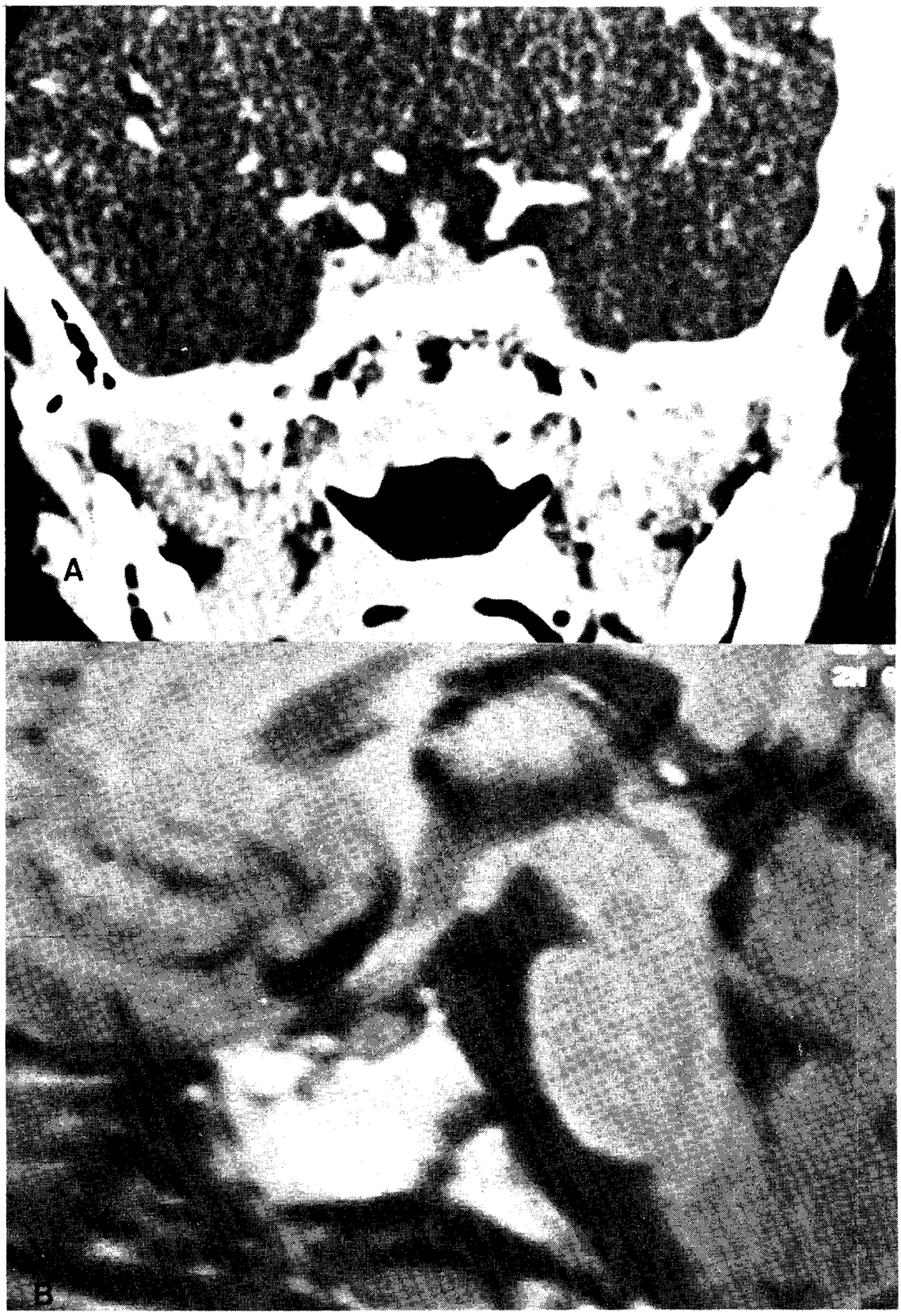

Fig. 5. Germinoma involving infundibulum and pituitary gland. Coronal view of post-contrast CT (A) shows small infundibular mass and upward convexity of the pituitary gland. Sagittal view of MR (SE 500/30) image (B) reveals enlargement of the infundibulum and pituitary gland with isointensity signal. Perisellar structures are better delineated on MR image (B).

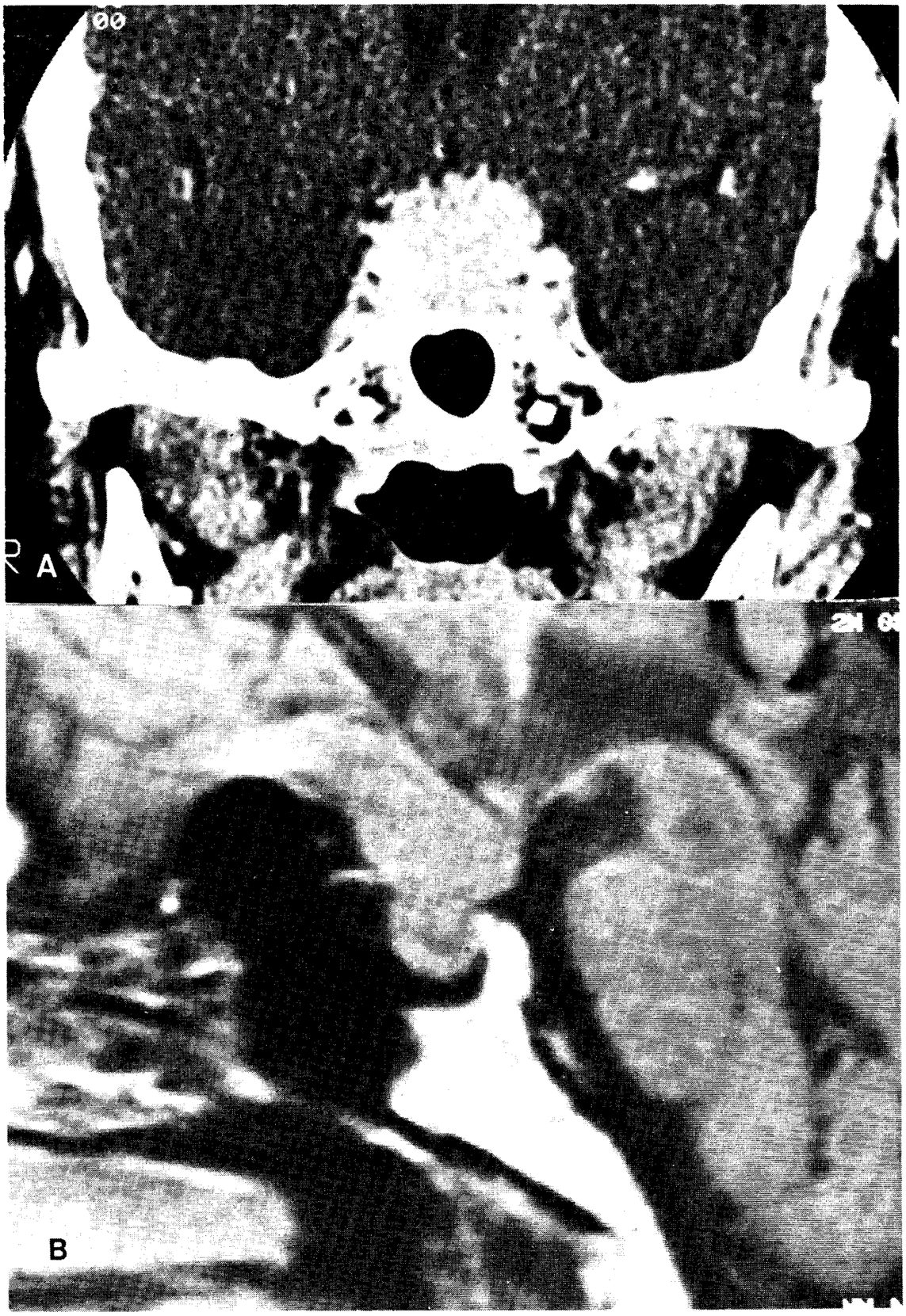

Fig. 6. Meningioma arising from tuberculum sella. Post-contrast CT (A) demonstrates well-defined homogeneously enhancing mass, while MR (SE 500/30) image (B) shows isointensity signal and poor differentiation from adjacent normal brain. Contrast resolution between the tumor and normal tissue is much better in CT.

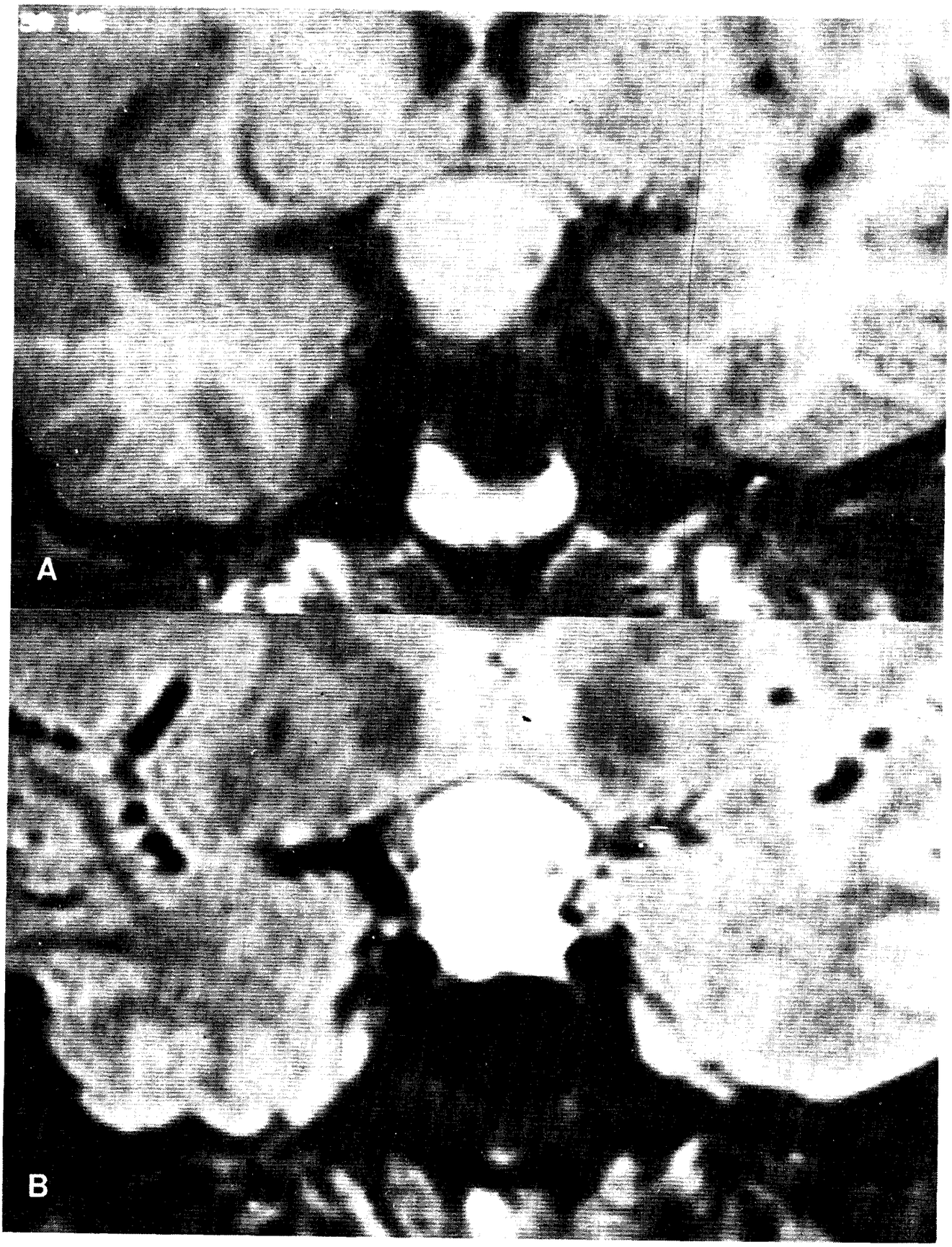

Fig. 7. Craniopharyngioma. The signal of the mass was slightly hyperintense on SE 500/30 image (A) and markedly hyperintense on SE 2000/60 image (B).

Fig. 8. Carotid-cavernous fistula, right. There is round area of signal void vascular structure within the right cavernous sinus on SE 500/30 image.

hyperintense on SE 500/30 and 2000/30 and markedly hyperintense on SE 2000/60 images (Fig. 7), while CT showed low attenuation, similar to cerebrospinal fluid (CSF) density in the suprasellar cistern. The extent of suprasellar extension was better evaluated using MR than CT because of the better contrast on the sagittal MR images.

MR imaging was superior in one CCF because it uniquely revealed the signal void vascular nature of the lesion in all sequences, whereas CT suggested an enhancing tumor (Fig. 8).

The signal of other suprasellar masses varied; a teratoma was markedly hyperintense in SE 500/30 and SE 2000/30 images, and mildly hyperintense in SE 2000/60 images. A trigeminal neuroma was isointense on SE 500/30, increasing slightly on SE 2000/60 sequence, and was slightly inhomogeneous. The central necrotic area with fluid-fluid level of low density on CT revealed marked hyperintensity in all sequences indicative of hemorrhagic necrosis. An epidermoid in the right parasellar area showed marked hypointensity on SE 500/30 and marked hyperintensity on SE 2000/60 like that of CSF. The tumor was slightly lobulated and inhomogeneous. The tumor of nasopharyngeal cancer with parasellar extension was isointense in all sequences of MR. CT better demonstrated the skull base bone destruction than MR. In a case of tuberculoma, the granuloma was isointense and slightly inhomogeneous, and was not separated from the surrounding edema on SE 500/30 images. SE 2000/30 and SE 2000/60 images demonstrated higher intensity of edema relative to isointense granuloma, allowing these to be discriminated. CT was superior to MR in contrast sensitivity in this case (Fig. 9).

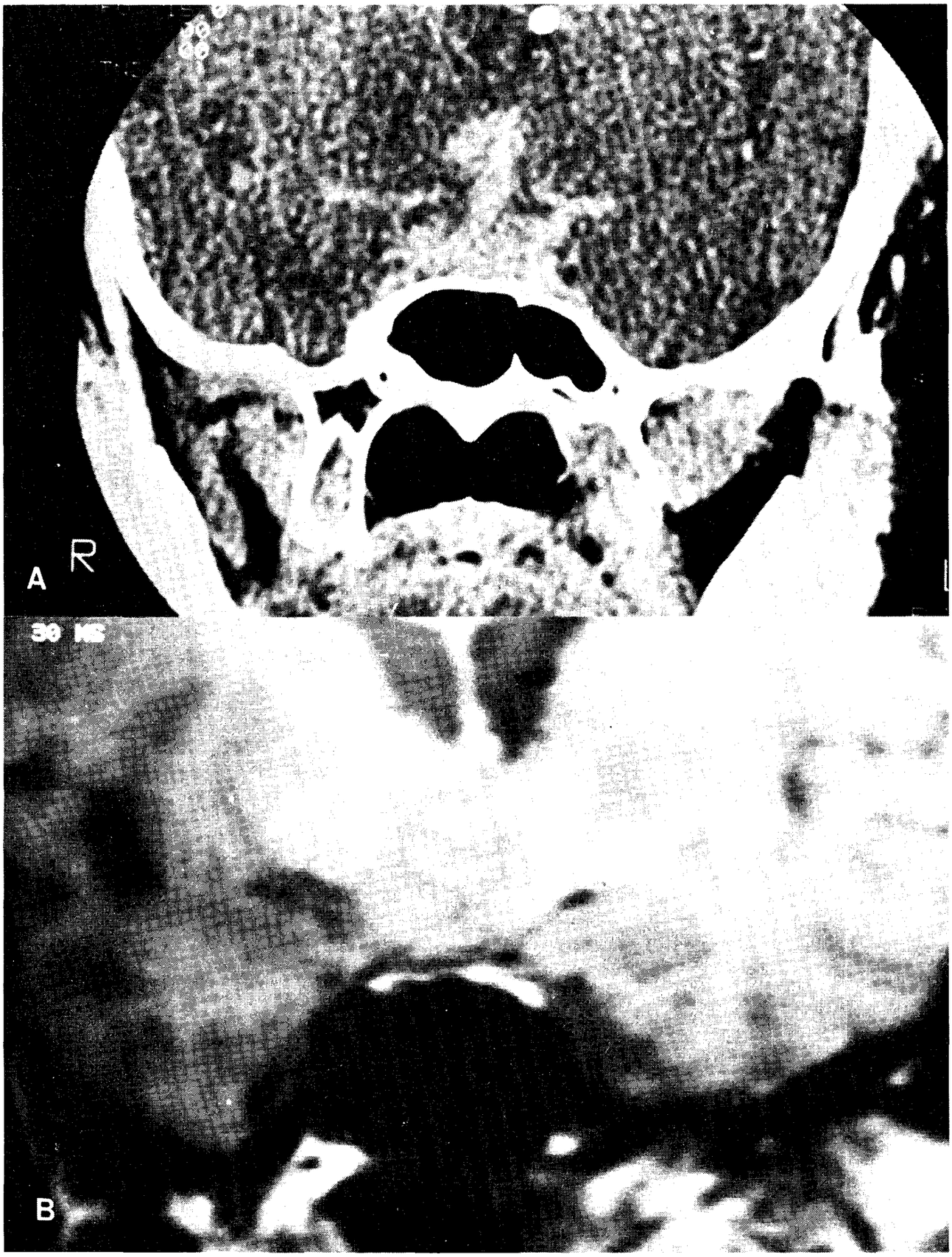

Fig. 9. Suprasellar tuberculoma. Post-contrast CT (A) reveals densely enhancing mass on suprasellar area, while MR (SE 500/30) image shows slightly inhomogeneous isointense mass at same area. Contrast resolution between the mass and normal tissue is better in CT.

DISCUSSION

MR imaging has significant advantages over CT. MR imaging permits better differentiation of lesions that are of similar low density on CT scans, as shown in cases of craniopharyngioma and hemorrhagic pituitary adenoma (Lee *et al.* 1985; Kucharczyk 1987). The sagittal MR image has better spatial resolution than reformatted CT scans and more accurately shows sellar enlargement caused by pituitary masses. MR also clearly demonstrates the relation of these lesions with the optic chiasm, infundibular stalk, and third ventricle. Coronal MR views are similar in resolution to direct coronal CT scans but are always free from artifacts and allow very precise delineation of lesions that arise from the hypothalamus and the foramen of Monro (Kucharczyk 1987).

Anatomic abnormalities from mass effect of macroadenomas were seen with both MR and CT. Most macroadenomas in this series were isointense with cortex on T1- or T2-weighted sequences. The normal gland was indistinguishable from adenomatous tissue. Use of paramagnetic contrast agents may improve the sensitivity of MR for adenoma detection (Davis *et al.* 1987). Abnormalities of the pituitary infundibulum were equally apparent with both imaging techniques. Cavernous sinus invasion was suspected more often with MR than with CT. The optic chiasm and chiasmal compression were well seen with MR, particularly with T1-weighted sequences. With CT, chiasmal compression was suspected based on the extent of a large suprasellar mass; however, the chiasm itself is not commonly visualized without metrizamide.

For microadenoma evaluation, MR is known to be not as sensitive as CT for identifying discrete focal lesions within the minimally enlarged or normal-sized pituitary gland, since an adenoma is a benign proliferation of a cell type normally found in the pituitary gland (Davis *et al.* 1987). But two cases of microadenoma in this series revealed high signal intensity, differing from normal pituitary gland. One microadenoma had been previously treated with bromocriptin. MR signal may change into high intensity in bromocriptine-treated adenomas owing to cellular changes rather than hemorrhage (Weissbuch 1986). Pojunas *et al.* (1986) reported that MR signals of microadenomas are variable in intensity. More experience with MR of microadenomas is necessary before any consistent pattern of MR findings can be identified. Identification of sellar-floor erosion was difficult with MR in patients with well-aerated sphenoid sinuses, due to the absence of signal from both air and calcium. Sellar-floor abnormalities were more readily seen with CT. At this time CT remains the imaging technique of choice for patients suspected of having a microadenoma (Davis *et al.* 1987). Further refinements in MR technique should be developed for the evaluation of small microadenomas.

The MR signal intensity of the germinomas is usually nearly isointense with that of the adjacent normal brain tissue (Kilgore *et al.* 1986). In this series, all three tumors revealed isointense signals, and in one infiltrating germinoma, the surrounding edema was demonstrated in balanced and T2-weighted sequneces as high intensity, but not in T1-weighted image. Even though MR better demonstrated the perisellar anatomic detal, CT seems to remain the procedure of choice for diagnosis of germ cell tumors because of poorer tumor contrast.

Meningiomas are generally slightly hypointense or isointense relative to cortex on T1-weighted images and isointense or hyperintense on T2-weighted images. A heterogeneous texture produced by tumor vascularity, calcifictions, cystic foci, or an intrinsic speckled or mottled pattern are usually observed in high field MR (Spagnoli *et al.* 1986). Spagnoli *et al.* (1986) also described that an interface between meningioma and brain was uniformly present and consisted of a cerebrospinal fluid cleft, vascular rim, or dural margin. In this series, signal intensity of two meningiomas is similar to those described, but in one tuberculum sellar meningioma, the interface between the tumor, optic chiasm and hypothalamus was not delineated. At surgery, the meningioma proved to be densely adhered to the surrounding brain tissue.

Unfortunately, many suprasellar abnormalities have similar signal intensities. By signal characteristics alone, MR imaging was nonspecific in the solid portion of macroadenomas, germinomas, meningiomas, trigeminal neuroma, nasopharyngeal cancer with parasellar extension and granuloma.

Craniopharyngiomas usually exhibited high signal on T2-weighted images (Lee *et al.* 1985; Karnaze *et al.* 1986; Pusey *et al.* 1987) and variable signal intensity on T1-weighted images (Pusey *et al.* 1987). Other lesions that appeared to be cystic on CT scans, such as the cystic portion of the pituitary adenomas in our series, had signal characteristics similar to or slightly higher than that

of CSF on T1-weighted sequence and could thus be differentiated.

The hyperintense signal of fat on T1-weighted images with decreasing signal intensity on longer sequences readily identifies fat-containing tumors such as teratomas. Recent hemorrhage with strong hyperintense signal on both T1- and T2-weighted images (Atlas *et al.* 1987), recognized in three hemorrhagic adenomas and in one trigeminal neuroma in our series, can be differentiated from fat tissue of teratomas.

Signal characteristics of epidermoid tumors varied with location of the tumor. Epidermoids in the cerebellopontine angle demonstrates signal intensity similar to that of CSF. These lesions had internal strand-like inhomogeneities (Latack *et al.* 1985; Newton *et al.* 1987).

Absent signal on all SE sequences caused by rapidly flowing blood, or absent signal on short TR/short TE images with augmentation of signal on longer TR/longer TE images from slow or turbulenet flow are findings that allow confident diagnosis of aneurysms and arteriovenous malformations. Confusion with tumors that show contrast enhancement on CT scans and subsequent diagnostic angiography can be avoided (Karnaze *et al.* 1986).

One of the limitations of CT is its inability to delineate the carotid arteries from sellar and juxtasellar masses in most cases. Because of blood flow, these arteries are seen normally as regions of little or no MR signal; displacement and compression can thus be readily observed. MR may be used instead of angiography to evaluate the carotid arteries and to exclude large aneurysms as a cause of sellar or juxtasellar lesions. Arteriography is still necessary for detailed evaluation of tumor vascularity.

Although both modalities allow detection of lesions equally well, CT is much better at depicting calcification (Zimmerman *et al.* 1985).

REFERENCES

Atlas SW, Grossman RI, Gomori JM, Hackney DB, Goldberg HI, Zimmerman RA, Bilaniuk LT. Hemorrhagic intracranial malignant neoplasms; Spin-echo MR imaging. Radiology 1987, 164:71-77

Bilaniuk LT, Zimmerman RA, Wehrli FW, Synder PJ, Goldberg HI, Grossman RI, Bottomley PA, Edelstein WA, Glover GH, MacFall JR, Redington RW. Magnetic resonance imaging of pituitary lesions using 1.0 to 1.5 T field strength. Radiology 1984a, 153:415-418

Bilaniuk LT, Zimmerman RA, Wehrli FW, Goldberg HI, Grossman RI, Bottomeley PA, Edelstein WA, Glover GH, MacFall JR, Redington RW, Kressel HY. Cerebral magnetic resonance; Comparison of high and low field strength imaging. Radiology 1984b, 153:409-414

Davis PC, Hoffman JC, Tindall GT, Braun IF. CT-surgical correlation in pituitary adenomas; Evaluation in 113 patients. AJNR 1985, 6:711-716

Davis PC, Hoffman JC, Spencer T, Tindall GT, Braun IF. MR imaging of pituitary adenoma; CT, clinical, and surgical correlation. AJNR 1987, 8:107-112

Karnaze MG, Sartor K, Winthrop JD, Gado MH, Hodges FJ. Suprasellar lesions; Evaluation with MR imaging. Radiology 1986, 161:77-82

Kilgore DP, Strother CM, Starshak RJ, Haughton VM. Pineal germinoma; MR imaging. Radiology 1986, 158:435-438

Kucharczyk W, Davis DO, Kelly WM, Sze G, Norman D, Newton TH. Pituitary adenomas; High-resolution MR imaging at 1.5 T. Radiology 1986, 161:761-765

Kucharczyk W. The pituitary gland and sella turcica. In Brant-Zawadzki M, Norman D (Ed) Magnetic resonance imaging of the certral nervous system. Raven Press, New York, 1987:pp. 187-208

Latack JT, Krtush JM, Kemink JL, Graham MD, Knake JE. Epidermoidomas of the cerebellopontine angle and temporal bone; CT and MR aspects. Radiology 1985, 157:361-366

Lee BCP, Deck MDF. Sellar and juxtasellar lesion detection with MR. Radiology 1985, 157:143-147

Newton TH. MRI of the epidermoid. Abstracts of 25th Annual Meeting of American Society of Neuroradiology. pp. 125-126

Oot R, New PFJ, Buonanno FS, Pykett IL, Kistler P, Delapaz R, Davis KR, Taveras JM, Brady TJ. MR imaging of pituitary adenomas using a prototype resistive magnet; Preliminary assessment. AJNR 1984, 5:131-137

Pojunas KW, Daniels DL, Williams AL, Haughton VM. MR imaging of prolactin-secreting microadenomas. AJNR 1986, 7:209-213

Pusey E, Kortman KE, Flanningan BD, Tsuruda J, Bradley WG. MR of craniopharyngiomas; Tumor delineation and characterization. AJNR 1987, 8:439-444

Spagnoli MV, Goldberg HI, Grossman RI, Bilaniuk LT, Gomori JM, Hackney DB, Zimmerman RA. Intracranial meniogiomas; High-field MR imaging. Radiology 1986, 161:369-375

Weissbuch SS. Explanation and implications of MR signal changes within pituitary adenomas after bromocriptine therapy. AJNR 1986, 7:214-216

Zimmerman RD, Fleming CA, Saint-Louis LA, Lee BC, Manning JJ, Deck MD. Magnetic resonance imaging of meningiomas. AJNR 1985, 6:149-157

＝ 국문초록 ＝

터키안 및 주위 병소에서의 고자장 (2.0T) 자기공명영상

서울대학교 의과대학 방사선과학교실, 신경외과학교실* 및 신경과학교실**

장기현 · 한문희 · 조병규* · 한대희* · 최길수* · 한만청 · 명호진** · 김주완

한국과학기술원에서 개발한 2.0 테스라의 초전도 자기공명영상장치를 이용하여 28예의 터키안 및 그 주위병소를 가진 환자에서 자기공명영상술 (MR)을 시행하여 그 영상을 전산화단층촬영 (CT)과 비교, 분석하였다. 대상 질환으로는 하수체 선종 14예, 배아세포종 3예, 수막종 2예, 공허 터키안 2예, 기타 두개인두종, 기형종, 유상피종, 삼차신경초종, 인두암의 두개강 침범, 결핵성 육아종, 경동맥 해면동루가 각각 1예씩 이었다.

MR은 시신경교차, 누루, 내경동맥, 제3뇌실, 해면동 등 터키안 주위의 구조물과 병소와의 관계를 CT보다 명확히 나타내주었으며, 특히 혈관성을 잘 나타내어 혈관 조영술을 일부의 환자에서는 생략할 수 있었다. MR은 또한 출혈부위, 지방조직 및 혈관의 특이소견을 보여 출혈성 종양과 경동맥 해면동루의 진단은 CT보다 용이하였다.

대조도에 있어서는 하수체 선종, 수막종, 배아세포종, 결핵성 육아종 등은 CT가 우월하였으나, 종양의 발견율은 비슷하였고, 석회화와 터키안저의 미란소견은 CT가 MR보다 예민하였다.